JOURNAL OF AIRCRAFT
Vol. 33, No. 2, March–April 1996

Control Issues for Rigid-in-Plane Helicopter Rotors

Amnon Katz* and Kenneth Graham†
University of Alabama, Tuscaloosa, Alabama 35487-0280

This article addresses an adverse control effect that arises in helicopter rotors when the following conditions occur: each blade is attached to the shaft through a single flapping hinge, there is no offset of the flapping hinges, the blades are constrained from leading or lagging, and the shaft maintains a strictly constant rate of rotation. When the rotor disk is tilted from the shaft, a bending moment is induced in the shaft that tends to further misalign the shaft and body from the rotor. The effect, which can amount to a control reversal, also applies to teetering rotors. The effect is derived analytically and corroborated by computer simulation. Two-blade rotors relieve the adverse effect by a two-per-rev fluctuation in the rate of rotation. The lesson for flight simulation is that a variable rate of rotation that responds to engine and rotor torque must be allowed in modeling rotor blade dynamics. In multiblade rotors the adverse effect cannot be relieved without lead/lag hinges. It can be overcome by offset flapping hinges.

Nomenclature

$\hat{e}$ = unit vector in direction of shaft bending moment
I, I' = definite integrals
J_b = blade moment of inertia
l_1 = height of rotor hub above c.g.
M_{fx} = total roll moment applied to fuselage
M_s = shaft bending moment
M_{sx} = roll component of shaft bending moment
M_{1x} = roll moment produced by tilted thrust
m = mass
r = distance from hub measured along the blade
t = time
$\boldsymbol{x}$ = radius vector, (x, y, z)
x = body system coordinate positive forward
y = body system coordinate positive to the right
Z = complex variable
z = body system coordinate positive down
β = blade flapping angle
τ = variable, place holder for tan ϕ
ϕ = lateral inclination of the disk relative to the shaft
Ω = angular velocity of the shaft
$\bar{\Omega}$ = average of Ω over a revolution

I. Introduction

THE purpose of this article is to point out an adverse moment that can arise in certain rotor configurations. The effect amounts to a control reversal for large lateral control inputs. It occurs when the following conditions hold:

1) Each blade is attached to the shaft through a single flapping hinge.

2) The flapping hinges are not offset from the shaft.

3) The blades are prevented from leading or lagging (rigid-in-plane).

4) The shaft maintains a strictly constant rate of rotation.

We observed this phenomenon in real-time man-in-the-loop flight simulation using the physically based dynamic blade model Bladehelo.[1,2] The ground rules were that the physical helicopter was to be simulated. No arbitrary adjustments for pilot acceptance were allowed. It was not our purpose to simulate the fine points of rpm control by the pilot. We therefore made the shaft rpm constant, as if a very effective governor were engaged. The adverse control effect resulted. The lesson for simulation technique was that the constant rpm mode was not permissible. Bladehelo was upgraded to determine rotor angular rate from the interplay of engine and rotor torque.

A qualitative explanation of the adverse effect, which is inertial in nature, is given in Sec. II. In Sec. III, the inertial lateral bending moment is computed analytically for a flat rotor disk inclined to the shaft. This computation represents the full inertial moment for a finite disk inclination in closed form. Some mathematical details are in Appendix A. Section IV compares the analytic results with computations performed with Bladehelo, which brings aerodynamic forces and moments into play, allows the blades flap and cone, and produces the inclination of the disk through cyclic pitch inputs. The results demonstrate that the adverse moment is the dominant inertial lateral bending moment and that it is virtually unchanged by aerodynamics and coning.

The numerical computation is applied to the Robinson R22, the configuration of which is closely approximated by Bladehelo with zero offset of the flapping hinge. The numerical results, which allow for aerodynamic forces and for coning, closely follow the analytical predictions. An analysis of the computational accuracy of Bladehelo is offered in Appendix B.

The adverse moment is of third order in ϕ. It is much smaller than the normal control moment for small ϕ. However, as the disk inclination ϕ (relative to the shaft) increases, the adverse moment grows faster than the normal moment. For the Robinson R22, the adverse moment catches up with the normal moment at a swashplate inclination of 8 deg, within the control authority of the lateral cyclic.

The adverse moment is a large-deflection effect. As such, it cannot be studied by small deflection expansion. A treatment valid for large deflections is required. The closed-form analysis of Sec. III and Appendix A and the Bladehelo model satisfy this criterion.

Section V discusses how the problem is avoided in practice and how it can be avoided in simulation. In the case of a two-blade rigid-in-plane configuration, the rotor maintains a constant rotational rate in its own plane, which translates into a two-per-rev fluctuation in the rate of rotation of the shaft. This relieves the adverse effect.

Where significant relief of the adverse moment is achieved by a ripple in the rotational rate, simulation must not postulate

Received Jan. 17, 1995; revision received Sept. 21, 1995; accepted for publication Sept. 25, 1995.

*Professor, Department of Aerospace Engineering, P.O. Box 870280. Member AIAA.

†Graduate Student, Department of Aerospace Engineering, P.O. Box 870280.

constant Ω. Rather, the free play of torque vs rotational rate must be simulated. In consequence of this study, Bladehelo was upgraded to include a mode in which engine torque, rather than rpm is prescribed (as determined by throttle input). Running in this mode, the R22 model produced no adverse moment.

In the case of multiblade rotors, the adverse effect cannot be fully relieved by a ripple in the rotational rate, but it can be overcome by offsetting the flapping hinges. When a hinge offset of a few degrees is introduced a favorable control moment is created that outweighs the adverse moment. A multiblade rotor can relieve the adverse effect with lead/lag hinges, or, in the absence of lead/lag hinges, can overcome the adverse control effect by having the (physical or virtual) flapping hinges offset from the hub.

The effect addressed here does not apply to arrangements where a universal joint is interposed between the rotor and the hub.

II. Qualitative Explanation

Figure 1 shows a flat rotor disk inclined to the shaft that carries it. Consider a blade, hinged to the shaft at the hub, that is free to flap, but is constrained from leading and lagging. The shaft is constrained to maintain a strictly constant rate of rotation. The projection of the blade on the plane perpendicular to the shaft moves at a constant angular velocity. A point on the blade actually slows down as the blade moves away from the reference plane. Like an ice skater who folds her arms, the rotation of the blades around the shaft would speed up, but is constrained by the absence of lead lag hinges. The blade applies a force to the shaft in the direction shown by an arrow in each of four quadrants.

The direction of the fore and aft component of the force in quadrant 1 is opposite to what it is in quadrant 2; the force in the longitudinal direction averages to zero over half a revolution. The lateral components in quadrants 1 and 2 add up. In both quadrants, the forces are directed to the right and are applied below the hub. In quadrants 3 and 4, the lateral forces are directed to the left and are applied above the hub. In this way, the forces average to zero over a revolution, but the moments add up. The forces shown by arrows in the rear view in Fig. 1 form a couple that introduces a bending moment into the shaft.

Note that flapping hinges, located at the hub, do not prevent the blades from applying a bending moment to the shaft. The shaft can be bent in two directions. The flapping hinges relieve only one of those.

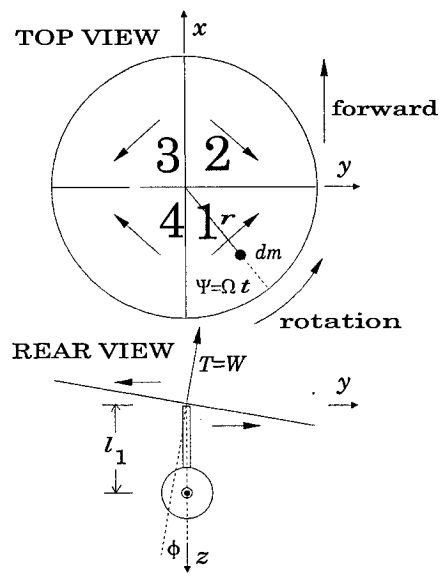

Fig. 1 Inclined disk and resulting moments.

The moment that the thrust of the inclined disk creates relative to the body c.g. tends to align the body with the rotor, i.e., make the shaft perpendicular to the rotor disk. This is the desired effect of tilting the rotor. The moment that the couple produced by blade inertia imparts to the hub tends to misalign the body from the rotor. It is an adverse phenomenon that diminishes or reverses the effect of the thrust moment.

III. Inertial Effect—Analytic Derivation

We are still addressing a flat disk (Fig. 1) with flapping hinges at the hub and no lead/lag hinges. The rotational rate of the shaft is a constant Ω. Consider a mass point on the blade of mass dm at a distance r from the hub. The relationship between ϕ and β is

$$\tan \beta = -\sin \Omega t \tan \phi \tag{1}$$

The trajectory of the point mass is

$$x = -r \cos \Omega t \cos \beta \tag{2}$$

$$y = r \sin \Omega t \cos \beta \tag{3}$$

$$z = -r \sin \beta \tag{4}$$

The in-plane components of velocity and acceleration of the point mass are

$$\dot{x} = \Omega r \sin \Omega t \cos \beta + r\dot{\beta} \cos \Omega t \sin \beta \tag{5}$$

$$\dot{y} = \Omega r \cos \Omega t \cos \beta - r\dot{\beta} \sin \Omega t \sin \beta \tag{6}$$

$$\ddot{x} = +\Omega^2 r \cos \Omega t \cos \beta - 2\Omega\dot{\beta} r \sin \Omega t \sin \beta + \dot{\beta}^2 r \cos \Omega t \cos \beta + r\ddot{\beta} \cos \Omega t \sin \beta \tag{7}$$

$$\ddot{y} = -\Omega^2 r \sin \Omega t \cos \beta - 2\Omega\dot{\beta} r \cos \Omega t \sin \beta - \dot{\beta}^2 r \sin \Omega t \cos \beta - r\ddot{\beta} \sin \Omega t \sin \beta \tag{8}$$

The values of $\dot{\beta}$ and $\ddot{\beta}$ in the previous equations are obtained by taking the derivative of Eq. (1):

$$\dot{\beta} = -\Omega \tan \phi \cos \Omega t \cos^2 \beta \tag{9}$$

$$\ddot{\beta} = \Omega^2(\tan \phi \sin \Omega t \cos^2 \beta - 2 \tan^2 \phi \cos^2 \Omega t \sin \beta \cos^3 \beta) \tag{10}$$

The inertial moment induced by the blade is $dm\, \ddot{x} \times x$. The component that is perpendicular to both the shaft axis and the flapping hinge is reacted by the shaft in bending. This component is in the direction of $\hat{e} = (-\cos \Omega t, \sin \Omega t, 0)$ and is given by the triple product $dm\, \ddot{x} \times x \cdot \hat{e}$. Expressed in terms of the components of the vectors, the shaft bending moment becomes

$$dM_s = dm \begin{vmatrix} \ddot{x} & x & -\cos \Omega t \\ \ddot{y} & y & \sin \Omega t \\ \ddot{z} & z & 0 \end{vmatrix} \tag{11}$$

When this determinant is developed by the last row, one finds

$$dM_s = dm\, \ddot{z} \begin{vmatrix} x & -\cos \Omega t \\ y & \sin \Omega t \end{vmatrix} + dm\, z \begin{vmatrix} -\cos \Omega t & \ddot{x} \\ \sin \Omega t & \ddot{y} \end{vmatrix} \tag{12}$$

The first determinant in Eq. (12) vanishes. In the second, all terms in $\ddot{x}$ and $\ddot{y}$ that are proportional to $-\cos \Omega t$ and $\sin \Omega t$, respectively, drop out. This leaves only the second term in Eqs. (7) and (8), and Eq. (12) easily evaluates to

$$dM_s = dm\ z2\Omega\dot{\beta}r \sin \beta \tag{13}$$

In the last equation, z is substituted from Eq. (4) and $\dot{\beta}$ from Eq. (9). Equation (1) may be reworked into

$$\cos^2\beta = \frac{1}{1 + \tan^2\phi \sin^2\Omega t} \tag{14}$$

$$\sin^2\beta = \frac{\tan^2\phi \sin^2\Omega t}{1 + \tan^2\phi \sin^2\Omega t} \tag{15}$$

When all of this is used, Eq. (13) becomes

$$dM_s = dm\ \Omega^2 r^2 \tan^3\phi \frac{\sin^2\Omega t \cos \Omega t}{(1 + \tan^2\phi \sin^2\Omega t)^2} \tag{16}$$

The next step is to integrate over the whole blade. One uses

$$\int dm\ r^2 = J_b \tag{17}$$

to obtain the shaft moment

$$M_s = J_b\Omega^2 \tan^3\phi \frac{\sin^2\Omega t \cos \Omega t}{(1 + \tan^2\phi \sin^2\Omega t)^2} \tag{18}$$

The instantaneous moment (18) is around an axis in the direction of $\hat{e} = (-\cos \Omega t, \sin \Omega t, 0)$. The pitch component of this moment averages to zero over a revolution. We are after the roll component, which is Eq. (18) times $-\cos \Omega t$. The result, averaged over a revolution and summed over all blades, is

$$M_{sx} = -n\Omega^2 J_b \tan^3\phi \frac{1}{2\pi} \int_0^{2\pi} \frac{\sin^2\Psi \cos^2\Psi}{(1 + \tan^2\phi \sin^2\Psi)^2} d\Psi \tag{19}$$

If the small angle approximation is applied to ϕ, then the denominator of the integrand becomes unity. The average of $\sin^2\Psi \cos^2\Psi$ evaluates to one-eighth, and one finds

$$M_{sx} = -(n/8)\Omega^2 J_b \phi^3 \tag{20}$$

A closed form of Eq. (19), without any approximation, is offered in Eq. (A11). However, it turns out that the leading correction to Eq. (20) is of the order ϕ^7; for $|\phi| < 10$ deg, Eq. (20) deviates from Eq. (A11) by less than 1:10^5. For this reason Eq. (20) was used to obtain the numerical results presented next.

The favorable rolling moment produced by the tilted disk at 1 g is

$$M_{1x} = Wl_1 \sin \phi \tag{21}$$

In this case the small angle approximation over the range $|\phi| < 10$ deg is good only to a little better than 1:100. In the plotted results that follow, we did not apply the small angle approximation to Eq. (21).

The total fuselage rolling moment is

$$M_{fx} = M_{1x} + M_{sx} \tag{22}$$

Figure 2 shows a plot of M_{fx} against ϕ. Figure 3 is a plot of M_{sx} against M_{fx}. The plots are based on the parameters of the Robinson R22 (Table 1). They show the control reversal occurring at about 8 deg of deflection. This is within the authority of the left lateral cyclic on the R22.

Table 1 Data for the Robinson R22 β

R = rotor radius, 151 in.
Ω = rotor rate of rotation, 53.404 rad/s
c = blade chord, 0.60 ft
blade twist, −7 deg
blade airfoil, 63−015
J_b = blade moment of inertia, 86.3 slug ft^2
n = number of blades, 2
W = gross weight, 1370 lb
l_1 = hub height above c.g., 6.00 ft

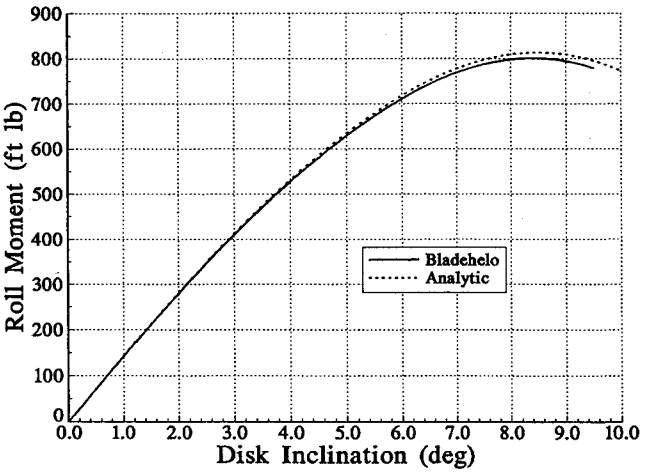

Fig. 2 Fuselage moment vs disk inclination.

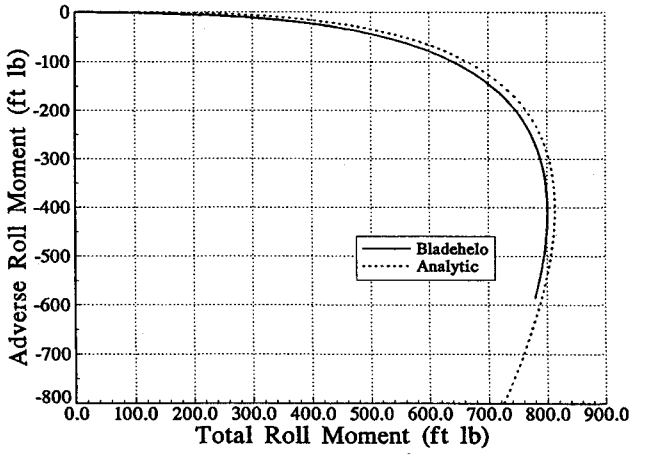

Fig. 3 Total moment and adverse moment.

IV. Computer Simulation

Together with the analytic results of the last section, Figs. 2 and 3 show the body moment and shaft (adverse) moment obtained by computer simulation. The simulation in question is Bladehelo, a rotor model developed at the University of Alabama, and featuring rigid blades that are free to flap, but cannot lead or lag.[1,2]

At the time of this writing Bladehelo has advanced beyond what is described in the references. It now allows for offset flapping hinges, with the amount of offset specified as input data. Besides the mode of constant shaft speed, a mode of operation at prescribed shaft torque is now available. In the man-in-the-loop simulation, the shaft torque is determined from the throttle input. However, the results shown in Figs. 2 and 3 were obtained with constant shaft speed and with the

hinge offset set to zero, in other words, with Bladehelo as described in Ref. 1.

The inputs into Bladehelo were selected to represent a Robinson R22 β (Table 1). Even though the Robinson features a unique three-hinge rotor configuration,[3] it was judged that Bladehelo correctly represents its properties that are significant to the current investigation. Like the Robinson, Bladehelo allows the individual blades to flap and cone; in both cases no moment parallel to the flapping hinge can be introduced into the shaft, both rotors are rigid-in-plane so that bending moments perpendicular to the flapping hinge are reacted by the shaft. The data in Table 1 came from Refs. 4 and 5, with Ref. 5 taking precedence.

The results in the figures were obtained with the shaft fixed and at rest relative to the airmass. Collective input was adjusted to produce a rotor thrust equal to the weight. This required a collective input of 12.55 deg. The resulting baseline condition represented hover out-of-ground effect. The lateral cyclic input was varied from 0 to 9.5 deg, the limit for the left lateral cyclic for the Robinson. A coning angle of 1.5 deg was formed. The inclination of the blade tip plane tracked the swashplate inclination within 0.03 deg.

It is seen that the full simulation closely bears out the analytic prediction of the control reversal phenomenon, based on inertia. An assessment of the accuracy of the numerical computation in Appendix B shows that the moments produced by Bladehelo are accurate to a fraction of a percent.

V. Discussion

The control reversal calculated in the previous sections does not occur with the Robinson or with other rigid-in-plane configurations such as the Bell teetering rotors. The prediction of control reversal is based on the assumption of a shaft rotating at a strictly constant rate. Actually, the rotational rate of the shaft is dominated by rotor inertia. This is especially true for a piston-engined helicopter such as the R22 with discrete cylinder firing. It is true also for turbine engines. It is rotor inertia that smooths the rotation to nearly constant rpm. However, because of inertia, the blades tend to maintain a constant rate of rotation in the plane of the tilted disk, which entails a 2Ω ripple in shaft angular velocity.

When this occurs, the inertial loads discussed in Secs. II and III disappear, and so does the adverse control moment. This is confirmed by Bladehelo, run in the prescribed torque mode rather than the constant rpm mode. The data is presented and compared in Fig. 4. The constant rpm data are the same as presented in Fig. 2. The prescribed torque data were obtained with the torque level regulated by a governor that responded to variations in Ω. The governor maintained Ω at the nominal value of Table 1, without suppressing the two-per-rev ripple in Ω. One sees that the adverse effect is not there. The analytic comparison data for this mode in Fig. 4 represent Eq. (21).

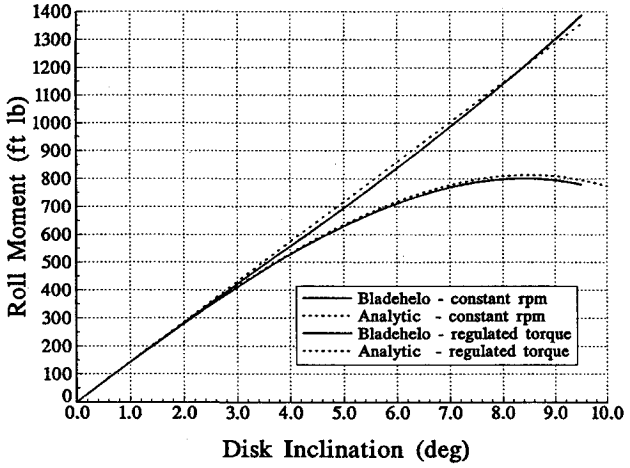

Fig. 4 Fuselage moment for constant Ω and for regulated torque.

The lesson for rotor simulation is that the assumption of constant shaft rate is unacceptable. The shaft speed must be allowed to vary with the interplay between engine torque and rotor torque. This level of fidelity is mandatory to reproduce handling qualities.

When the flapping hinges are offset, a favorable shaft moment is induced that masks the adverse moment. A rotor on a constant speed shaft is not then uncontrollable. Nevertheless, handling qualities are still misrepresented.

Transmission and engine inertia tend to oppose the relief of the inertial adverse effect. They are normally too small to be significant. Blade in-plane flexibility should have a slight beneficial effect. Governors that maintain shaft speed are not effective in smoothing the 2Ω ripple. If a governor design that could achieve this were practical, it must be avoided, or the control reversal predicted here would occur.

Note that the relief of the inertial adverse effect by fluctuations in the rate of rotation is possible only with two-blade rotors. Multiblade rotors cannot fully relieve the effect. In particular, four-blade rotors, with blades equally spaced, are subject to the full effect, since the torques produced by one pair of opposing blades is canceled by the other. Indeed, it was in the context of a four-blade rotor that De La Cierva introduced the lead/lag hinges.

Cierva was thinking of structural effects. In the real world, structural stress and fatigue in the blades and in the shaft accompany the adverse bending. In simulation, we permit ourselves to overlook such details. The structural effects are well known, but the control implications are not. In this way, Prouty (Ref. 4, pp. 145 and 146) states that lead/lag hinges are there for structural reasons, and that no control issues are involved. We have shown, to the contrary, that significant control problems do arise. Once the rotor has failed structurally, the issue of controlling it becomes moot. However, advances in structural technology have made rigid rotors practical.

A multiblade rotor design can relieve the adverse control effect by use of lead/lag hinges. It can overcome the adverse effect by offset of the (physical or virtual) flapping hinges from the hub. A universal joint between the hub and rotor may also serve to relieve the adverse control moment. With the absence of any of these—lead/lag hinges, offset flapping hinges, or a universal joint—a multiblade rotor would be subject to deterioration of control authority with disk inclination, amounting at some point to a control reversal.

Appendix A: Closed-Form Revolution Average

In this Appendix, the definite integral in Eq. (19)

$$I = \frac{1}{2\pi}\int_0^{2\pi} \frac{\sin^2\Psi \cos^2\Psi}{(1 + \tau^2 \sin^2\Psi)^2}\, d\Psi \tag{A1}$$

is evaluated analytically by use of the Cauchy integral theorem. In Eq. (A1), $\tan\phi$ was replaced by a variable τ. This is done for brevity in the following manipulations.

We start by introducing a new variable of integration:

$$Z \equiv \sin\Psi \tag{A2}$$

It follows that

$$dZ = \cos\Psi\, d\Psi \tag{A3}$$

$$\cos\Psi = \sqrt{1 - Z^2} \tag{A4}$$

With these substitutions Eq. (1) is transformed into

$$I = \frac{1}{2\pi}\oint_C dZ \frac{Z^2\sqrt{1 - Z^2}}{(1 + \tau^2 Z^2)^2} \tag{A5}$$

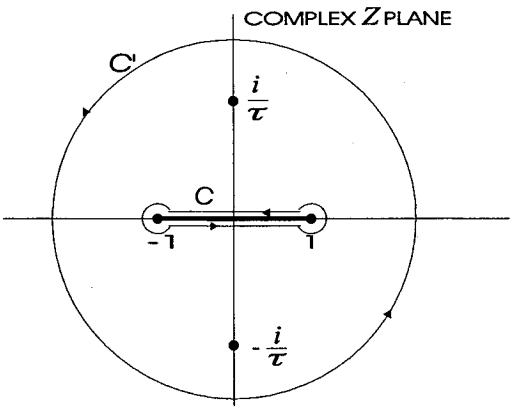

Fig. 5 Integration contours in the complex plane.

The integrand is a meromorphic function in the complex Z plane with a slit running between -1 and 1 and poles at $Z = \pm i/\tau$. The integral is over a contour C that hugs the slit (Fig. 5).

Now deform the contour of integration into the large circle C' (Fig. 5). In the process the contour has crossed the two poles. The integral I is now over C', less the contribution of the two poles.

The integral over C' is evaluated by expanding the integrand in powers of $1/Z$:

$$I' = \frac{i}{2\pi}\frac{1}{\tau^4}\oint_{C'}\frac{dZ}{Z}\frac{\sqrt{1-(1/Z^2)}}{[1+(1/\tau^2Z^2)]^2}$$
$$= \frac{i}{2\pi}\frac{1}{\tau^4}\oint_{C'}\frac{dZ}{Z}(1+\cdots) = -\frac{1}{\tau^4} \tag{A6}$$

The residue at the double pole at $Z = i/\tau$ is given by

$$R = \frac{1}{2\pi\tau^4}\left[\frac{d}{dZ}\frac{Z^2\sqrt{1-Z^2}}{(1+\tau^2Z^2)^2}\right]_{Z=i/\tau} \tag{A7}$$

The computation of this expression is straightforward, if slightly tedious, and the contribution to the integral becomes

$$2\pi iR = -\frac{1}{2\tau^4}\frac{1+\frac{1}{2}\tau^2}{\sqrt{1+\tau^2}} \tag{A8}$$

The contribution of the other pole is equal. In this way finally

$$I = I' - 4\pi iR = \frac{1}{\tau^4}\left(\frac{1+\frac{1}{2}\tau^2}{\sqrt{1+\tau^2}} - 1\right) \tag{A9}$$

Equation (A9) is the closed-form expression of Eq. (A1). When this is used in Eq. (19), with $\tan\phi$ substituted for τ, the rigorous counterpart of Eq. (18) becomes

$$M_{sx} = n\Omega^2 J_b \frac{1}{\tan\phi}\left(1 - \frac{1+\frac{1}{2}\tan^2\phi}{\sqrt{1+\tan^2\phi}}\right) \tag{A10}$$

Table B1 Accuracy comparisons

Steps per revolution	Fuselage moment, ft × lb, %	Adverse moment, ft × lb, %
92	779.36	−584.85
920	777.24	−585.10
Error	2.12	0.25
Percent	0.27	0.04

Collective input = 12.55 deg and cyclic input = −9.5 deg.

The last expression can be streamlined by exploiting trigonometric identities to read

$$M_{sx} = n\Omega^2 J_b \frac{\cos\phi + \frac{1}{2}\sin^2\phi - 1}{\sin\phi} \tag{A11}$$

The properties of Eq. (A11) are not obvious upon inspection, since both numerator and denominator vanish as ϕ tends to zero. An expansion in powers of ϕ yields

$$\frac{\cos\phi + \frac{1}{2}\sin^2\phi - 1}{\sin\phi} = -\frac{1}{8}\phi^3 + \frac{17}{5760}\phi^7 + \cdots \tag{A12}$$

In leading order, Eq. (A11) is identical to Eq. (20). The first correction to Eq. (20) is of order ϕ^7, i.e., order of ϕ^4 smaller than the leading term. With $|\phi|$ smaller than 10 deg (0.175 rad), Eqs. (20) and (A11) agree to better than $1{:}10^5$.

Appendix B: Accuracy of the Computer Simulation

The results plotted in Figs. 2 and 3 were obtained with 92 integration steps per revolution. In Table B1, the values of fuselage roll moment and shaft roll moment with a full left cyclic input (9.5 deg) obtained this way are compared to values obtained with 920 integration steps per revolution. The difference of the results serves as an estimate of the integration error. It is seen that the moments computed at 92 steps per revolution are accurate to a fraction of a percent.

Acknowledgments

Kenneth Graham would like to acknowledge support by the NASA Langley Research Center through a Graduate Student Researcher Grant NGT-51245. The authors are indebted to R. Prouty for helpful comments.

References

[1]Graham, K., and Katz, A., "A Blade Element Model in a Low Cost Helicopter Simulator," *Proceedings of the AIAA Flight Simulation Technologies Conference* (Scottsdale, AZ), AIAA, Washington, DC, 1994, pp. 287–293 (AIAA Paper 94-3436).

[2]Katz, A., "Performance Benefit of Second Harmonic Control in Helicopters," *Journal of Aircraft*, Vol. 32, No. 2, 1995, pp. 442, 443.

[3]Robinson, F. D., "Rotor Hub and Oil Seal," U.S. Patent 4,131,391, Dec. 26, 1978.

[4]Prouty, R. W., *Helicopter Performance, Stability, and Control*, Krieger, Malabar, FL, 1990, p. 696.

[5]"R22 Pilot's Operating Handbook and FAA Approved Rotorcraft Flight Manual, RTR 061," Robinson Helicopter Co., Torrance, CA, March 1979, revised Feb. 4, 1993.